IAI Accepted Manuscript Posted Online 9 January 2017
Infect. Immun. doi:10.1128/IAI.00930-16

Infection and Immunity

Quorum sensing regulators are required for metabolic fitness in *Vibrio parahaemolyticus*

Sai Siddarth Kalburge[a], Megan R. Carpenter[a], Sharon Rozovsky[b] and E. Fidelma Boyd[a]#

Department of Biological Sciences, University of Delaware, Newark, DE 19716[a]

Department of Chemistry and Biochemistry, University of Delaware, Newark, Delaware, 19716, United States[b]

Running title: quorum sensing regulators, carbon metabolism and transport, *Vibrio parahaemolyticus* intestinal colonization

#Corresponding author: E. Fidelma Boyd – fboyd@udel.edu

Department of Biological Sciences, 328 Wolf Hall, University of Delaware,
Newark, DE 19716

Phone: (302) 831-1088. Fax: (302) 831-2281

Abstract

Quorum sensing (QS) is a process by which bacteria alter gene expression in response to cell density changes. In *Vibrio* species, at low cell density, the sigma 54-dependent response regulator LuxO, is active, and regulates the two QS master regulators AphA, which is induced and OpaR, which is repressed. At high cell density the opposite occurs, LuxO is inactive, therefore OpaR is induced and AphA is repressed. In *V. parahaemolyticus,* a significant enteric pathogen of humans, the role of these regulators in pathogenesis is less known. We examined deletion mutants of *luxO, opaR* and *aphA* for *in vivo* fitness using an adult mouse model. We found that the *luxO* and *aphA* mutants were defective in colonization compared to wild-type. The *opaR* mutant did not show any defect *in vivo*. Colonization was restored to wild-type levels in a *luxO/opaR* double mutant and was also increased in an *opaR/aphA* double mutant. These data suggest that AphA is important and that overexpression of *opaR* is detrimental to *in vivo* fitness. RNA-seq analysis of the wild-type and *luxO* mutant grown in mouse intestinal mucus showed that 60% of the genes that were downregulated in the *luxO* mutant were involved in amino acid and sugar transport and metabolism. These data suggest that the luxO mutant has a metabolic disadvantage, which was confirmed by growth pattern analysis using phenotype microarrays. Bioinformatics analysis revealed OpaR binding sites in the regulatory region of 55 carbon transporter and metabolism genes. Biochemical analysis of five representatives of these regulatory regions demonstrated direct binding of OpaR in all five tested. These data demonstrate the role of OpaR in carbon utilization and metabolic fitness, an overlooked role in the QS regulon.

Introduction

Vibrio parahaemolyticus is the leading cause of bacterial seafood borne gastroenteritis worldwide resulting in mild to severe inflammatory gastroenteritis (1-5). The completed genome sequence of *V. parahaemolyticus* RIMD2210633, an O3:K6 serotype associated with pandemic disease, demonstrated the presence of two type III secretion systems (T3SSs) one on each chromosome, which led to the identification of several effector proteins associated with inflammatory diarrhea (6-8). Studies have shown that T3SS-2 is the major contributing factor towards enterotoxicity and that inflammatory diarrhea and intestinal epithelium cell disruption are dependent upon a functional T3SS-2 (9-12).

Much less is known about how *V. parahaemolyticus* initially colonizes and survives within the host gastrointestinal tract. This lack of knowledge is in part due to a lack of animal models to study colonization and infection *in vivo*. The development of a streptomycin pretreated adult mouse model that removes microbiota colonization resistance and allows *V. parahaemolyticus* to colonize has uncovered a number of bacterial colonization factors required for colonization (13-15). Examination of a mutant deficient in the global regulator ToxR demonstrated a significant defect in intestinal colonization compared to the wild-type (13). This study showed that ToxR was a negative regulator of the global regulator LeuO and a positive regulator of T3SS-1 and the major outer membrane porin OmpU (13). OmpU was shown to be essential for resistance and tolerance to acid and bile salts, important abiotic stresses *in vivo* (13). The importance of ToxR for *in vivo* survival also was demonstrated in an infant rabbit model of infection (16). The alternative sigma factor RpoE, required for the cell envelope stress response, was shown to be essential for *in vivo* survival, as deletion of the *rpoE* gene resulted in attenuation of mouse colonization (15). In contrast, analysis of a deletion mutant of sigma-54,

rpoN showed that in *in vivo* competition assays, the mutant colonized significantly more proficiently than the wild-type strain. The mechanism for the enhanced colonization of the *rpoN* mutant is unknown, however, it was shown that the *rpoN* mutant had a metabolic advantage over wild-type when grown in intestinal mucus and its components. Expression analysis showed that genes required for gluconate, ribose and arabinose catabolism were induced in the *rpoN* mutant. These data suggested that specific carbon metabolism genes are negatively regulated by RpoN and that competitive carbon utilization could be an important colonization factor (14).

Quorum sensing is a process by which bacteria modulate gene expression in response to cell density changes and is mediated by autoinducers such as acyl homoserine lactone that act as extracellular signals (17-22). Quorum sensing has been studied in a number of *Vibrio* species including *V. parahaemolyticus,* which contains the central conserved components of the quorum sensing pathway identified in *V. harveyi* (**Fig. 1**) (22-34). In *V. harveyi*, quorum sensing regulation of gene expression is carried out by two quorum sensing master regulators, the low cell density (LCD) regulator AphA and the high cell density (HCD) regulator, LuxR. At LCD, when the autoinducer concentration is low, LuxO, the QS response regulator is active and functions as an activator for sigma factor RpoN (δ^{54}) that then aids in the transcription of five small RNAs termed quorum regulatory RNAs (*qrr*) 1-5(35, 36). Qrrs are bacterial sRNAs that are partially complimentary to their target mRNA and thereby regulate gene expression post-transcriptionally. They require the sRNA chaperone Hfq for their activity (36-38). Qrrs were identified first in *V. cholerae* where they were shown to repress HapR (the LuxR homologue) through direct base pairing (37). The Qrrs stabilize the mRNA of *aphA* and destabilize the mRNA of *luxR*. In addition, AphA represses *luxR* transcription, independent of the Qrrs (36, 39, 40). At HCD, LuxO is not active, the *qrrs* are not transcribed, leading to a constitutively

93 expressed LuxR, which in turn represses the transcription of *aphA* (**Fig. 1**) (36, 39, 40). The *V.*
94 *parahaemolyticus* genome contains each of the components described above, *luxO, qrr1* to *qrr5,*
95 *aphA* and *opaR,* the *luxR* homologue in this species (25, 30, 37, 41, 42 Zhang, 2012 #25). LuxR
96 and OpaR regulate 100s of genes in *V. harveyi* and *V. parahaemolyticus,* respectively (30, 39,
97 42). OpaR was shown to positively regulate capsule polysaccharide (CPS) production,
98 competence, and type VI secretion system-2 (T6SS-2) production and negatively regulate
99 motility, biofilm, and T3SS-1 and T6SS-1 production (30, 32-34, 41-43). AphA was shown to
100 regulate several genes in various *Vibrio* species including genes involved in biofilm formation,
101 motility and virulence (39, 44-46). In *V. harveyi*, AphA coregulated a number of genes including
102 the T3SS apparatus along with LuxR (39). In *V. parahaemolyticus*, AphA is required for
103 motility, biofilm formation and an *aphA* mutant strain is avirulent in a murine infection model
104 (41).

105 In this study, we determined the role of the QS regulators in *V. parahaemolyticus*
106 intestinal colonization, the first step in pathogenesis. We constructed a *luxO* deletion mutant and
107 *in vivo* analysis showed that the mutant had a significant defect in a streptomycin pretreated adult
108 mouse model of colonization. We determined whether the defect in the *luxO* mutant was through
109 its regulation of the QS regulators OpaR or AphA by constructing deletions in each of these
110 genes as well as double deletion mutants and examined the *in vivo* phenotypes. The *aphA* mutant
111 was attenuated for colonization similar to the *luxO* mutant, whereas the *opaR* mutant showed no
112 defect in colonization. Double deletion mutants *luxO/opaR* and *opaR/aphA* showed significantly
113 increased colonization abilities compared to the single *luxO* or *aphA* deletion mutants. These
114 results suggested that AphA is important for *in vivo* fitness likely in part through its negative
115 regulation of *opaR* and that over expression of *opaR* is detrimental. Comparative transcriptome

analysis of wild-type versus the *luxO* mutant grown in mouse intestinal mucus showed 60% of genes downregulated in the *luxO* mutant were involved in metabolism. Using phenotype microarrays, we found significant differences in growth between the wild-type and *luxO* and *aphA* mutant strains in 25 carbon sources. Bioinformatics analysis identified putative OpaR binding sites in the regulatory regions of carbon metabolism and transporter genes. By using electrophoretic mobility shift assays, we show direct binding to five of these regulatory regions. Overall, the data demonstrate a direct role for the QS regulator OpaR in cell metabolism and suggests a mechanism for the *in vivo* phenotypes of the *luxO* and *aphA* mutants.

Material and Methods

Bacterial strains, media and culture conditions. All the strains and plasmids used in this study are listed in **Table S1**. A streptomycin-resistant strain of *V. parahaemolyticus* O3:K6 clinical isolate RIMD2210633 was used throughout this study (13, 47). For competition experiments a β-galactosidase-positive strain of RIMD2210633, named WBWlacZ was used.Colonies of the WBWlacZ strain appear blue on an X-gal plate in comparison to the wild-type and its isogenic mutants that appear white on the plate, thus allowing for a blue: white screen in a competition experiment. The WBWlacZ was previously shown to behave identical to wild-type *in vitro* and *in vivo* (13, 14). Unless stated otherwise, all *V. parahaemolyticus* strains were grown in Lysogeny Broth (LB) containing 3% NaCl (LBS) (Fischer Scientific, Pittsburgh, PA) at 37°C with aeration. For growth studies, M9 medium (Sigma Aldrich, St. Louis, MO) supplemented with 3% NaCl was used to which different carbon sources were added. For genetic manipulations, an *Escherichia coli* diaminopimelic acid (DAP) auxotroph β2155 λpir was used.

138 The *E. coli* β2155 λpir strain was cultured in LB medium supplemented with 0.3 mM DAP
139 (Sigma Aldrich). When required, antibiotics were used at the following concentrations:
140 streptomycin, 200 µg/ml; chloramphenicol, 25 µg/ml; ampicillin 100 µg/ml.

141 **Construction of *V. parahaemolyticus* RIMD2210633 quorum sensing deletion mutants.**
142 Splicing by overlap extension (SOE) PCR with homologous recombination (48) was used to
143 construct in-frame nonpolar deletions in VP2099 (*luxO*), VP2762 (*aphA*), VP2516 (*opaR*) and
144 double deletion mutants *luxO/opaR* and *opaR/aphA* as previously described by this group (13-15,
145 47, 49). Primers were designed to the QS response regulator *luxO* and the two QS master
146 regulators *opaR* and *aphA* using the *V. parahaemolyticus* RIMD2210633 genome sequence as
147 the template. All primers used in the study are listed in **Table S2** and SOE PCR was performed
148 to obtain a 75-bp truncated version of the 1,362-bp *luxO* gene, a 39-bp truncated version of the
149 615-bp *opaR* gene and a 48-bp truncated version of the 540-bp *aphA* gene. All mutants were
150 confirmed by PCR analysis and were verified to be in-frame by sequencing.

151 ***In vivo* competition assays.** All experiments involving mice were approved by the University of
152 Delaware Institutional Animal Care and Use Committee. Male C57BL/6 mice, aged 6 to 10 wk
153 were housed under specific-pathogen-free conditions in standard cages in groups (4 or 5 per
154 group) and provided standard mouse feed and water *ad libitum.* Streptomycin pre-treatment and
155 inoculations were performed as previously described (13, 14). Briefly, 24 h before bacterial
156 inoculations by oral gavage, mice were fasted for 4 h and then administered 20 mg streptomycin
157 per animal orogastrically and then food and water were immediately returned. Four hours prior
158 to inoculation food and water were removed. Water was restored immediately upon inoculation
159 and food was restored 2 h post-infection. The *V. parahaemolyticus* strain used for *in vivo*
160 experiments is the β-galactosidase knock-in designated WBWlacZ, which allows for a blue:white

161 colony screening (13-15). Overnight cultures were diluted 1:50 with LBS streptomycin media
162 and grown for 4 h at 37°C with aeration. An aliquot of the 4 h culture was pelleted and
163 resuspended in PBS to a final concentration of ~1×10^{10} CFU/ml. A 1 ml aliquot of each deletion
164 mutant strain was combined with 1 ml of the WBWlacZ strain, yielding a bacterial suspension of
165 ~1×10^{10} CFU/ml with a ratio of 1:1 CFU of mutant to WBWlacZ strain. Mice were inoculated
166 with 100 µl of the appropriate bacterial suspension. An aliquot of the inoculum was serially
167 diluted and plated onto LBS plates with streptomycin and X-gal in order to determine the exact
168 ratio of CFUs in the inoculum. For *in vitro* competition assays, a 100 µl aliquot of the *in vivo*
169 inoculum was added to 5 ml of LBS, grown at 37°C with aeration for 24 h and serially diluted
170 and plated. The mice were sacrificed 24 h post infection and the gastrointestinal tract was
171 harvested and suspended in 8 ml of sterile PBS, homogenized mechanically, serially diluted and
172 plated on LBS plates containing 120 µg/ml X-gal and incubated at 37°C overnight. The
173 competitive index (CI) for the *in vivo* and *in vitro* assays was determined with the following
174 equation: CI = ratio $out_{(mutant/wild\text{-}type)}$/ratio $in_{(mutant/wild\text{-}type)}$. A CI >1 indicates that the test strain
175 has the ability to out-compete the wild-type strain, while a CI of <1 indicates that the test strain
176 is less fit than the wild-type strain.

177 **Capsule polysaccharide (CPS) production and biofilm assays.** CPS production was examined
178 using heart infusion (HI) (Remel, Lenexa, KS) plates containing 1.5% agar, 2.5 mM $CaCl_2$, and
179 0.25% Congo red dye. Single colonies were inoculated onto the surface of the plates and were
180 incubated at 30°C for 36 h before images were taken. Biofilm formation was examined using the
181 crystal violet assay. Briefly, overnight cultures of *V. parahaemolyticus* were diluted 1:40 into
182 LBS and grown statically in 96-well strip plates at 37°C for 3, 6, 12 and 24h. After static
183 incubation, the culture was decanted from each well and the well was washed once with sterile

184 phosphate buffered saline (PBS). Crystal violet was added into each well and the plate was
185 incubated at room temperature for 30 min. The crystal violet was decanted out and the well was
186 washed with sterile PBS. The PBS was then decanted out and crystal violet that had stained the
187 adherent cells was solubilized completely in dimethylsulfoxide (DMSO) and the optical density
188 (OD_{595}) was measured to quantify the amount of biofilm formed.

189 **RNA extraction, Illumina sequencing and quantitative real time PCR (qPCR)**. *Vibrio*
190 *parahaemolyticus* wild-type and mutant strains were grown for 4 h in LBS and then diluted 1:50
191 into M9 medium supplemented with mouse intestinal mucus as the sole carbon source and the
192 cells were grown statically. We examined early-exponential-phase cultures that were grown for
193 1.5 h, considering the low cell density condition would restrict *opaR* levels in the wild-type,
194 thereby allowing us to observe the greatest difference in *opaR* levels between the *luxO* mutant
195 and wild-type. Total RNA was extracted from cells obtained by centrifugation at the end of 1.5 h
196 using Trizol (Invitrogen, Carlsbad, CA) according to manufacturer's protocol. The RNA samples
197 were then quantified using a Nanodrop spectrophotometer (Thermo Scientific, Waltham, MA).
198 The samples were treated with Turbo DNase (Invitrogen) according to manufacturer's
199 instructions. For each sample of the wild-type and mutant, RNA samples from two independent
200 cultures were pooled together. Nanodrop quantifications were used to ensure equal
201 representation of RNA from both biological replicates. Then, 3 µg of RNA was used for rRNA
202 depletion using the Ribo-Zero rRNA removal kit for Gram-negative bacteria (Illumina, San
203 Diego, CA). Libraries for each sample were prepared from 100ng of rRNA-depleted-RNA using
204 the Illumina TruSeq Stranded mRNA kit (Illumina). Sequencing was performed at the University
205 of Delaware Sequencing and Genotyping Center on the HiSeq 2500 platform to yield 51-base
206 single-end reads.

207 For qPCR validations of the RNA-Seq, 500 ng of pre-ribozero treated RNA was used as a
208 template for cDNA synthesis. cDNA was synthesized using Superscript III reverse transcriptase
209 (RT) (Invitrogen) following manufacturer instructions using 500 ng of RNA template and
210 priming with 200 ng of random hexamers. cDNA samples were then diluted 1:25 and used for
211 quantitative-real time PCR (qPCR). To analyze expression of the wild-type and mutant strains at
212 HCD, cells were grown for 4 h in LBS medium and were then diluted 1:50 into M9 medium
213 containing 3% NaCl and supplemented with glucose (M9G) and grown to an OD of 1.0. Total
214 RNA was extracted using the Trizol extraction protocol detailed above. 500 ng of the DNase
215 treated RNA samples were used as template for cDNA synthesis. cDNA samples were then
216 diluted 1:25 or 1:10 and used for quantitative-real time PCR (qPCR). Fast SYBR Green master
217 mix or PowerUp SYBR Green master mix (Life Technologies, Carlsbad, CA) was used for
218 qPCR and samples were run on an Applied Biosystems 7500 fast real-time PCR system or
219 QuantStudio 6 Flex real-time PCR system (Applied Biosystems, Foster City, CA). Each
220 experiment was performed in duplicate with at least two biological replicates. Primers used for
221 the qPCR reactions are listed in **Table S2**. Data was analyzed using Applied Biosystems
222 software. Expression levels of each gene as determined by their cycle threshold (C_T) values,
223 were normalized using the 16s rRNA housekeeping gene to correct for sampling errors.
224 Differences in the ratios of gene expression were determined using the $\Delta\Delta C_T$ method (50).

225 **RNA-Seq analysis**. Raw 51-base reads were filtered to remove adaptor only sequences and low
226 quality reads using the FASTX Toolkit. Filtered reads were aligned to the *V. parahaemolyticus*
227 RIMD2210633 genome (Refseq ID NC_004603.1 Chromosome 1 and NC_004605.1
228 Chromosome 2) using Burrows-Wheeler Aligner (BWA.aln) version 0.7.7. Gene annotations
229 were obtained from Ensembl bacteria, Rfam, Bacterial Small Regulatory RNA database and

230 RAST. Number of reads aligning to each genomic position were calculated using Htseq version
231 0.6.1. Differential expression analysis was performed on obtained read counts using DESeq2
232 version 1.4.5. Differential expressed genes were categorized into Cluster of orthologous groups
233 (COG) obtained from Integrated Microbial Genomes (IMG) database.

234 **Growth analysis and *in vitro* competition assays.** Strains were grown overnight in M9G at
235 37°C with aeration. For the Biolog PM1 and PM2A phenotype microarrays (Biolog Inc.,
236 Hayward, CA), overnight cultures were then diluted 1:50 into fresh M9G and allowed to grow
237 for 4 h. These cultures were pelleted by centrifugation for 10 min at 4,000 x *g*, washed twice
238 with PBS and then diluted 1:50 into fresh M9 media supplemented with 3% NaCl and 100 µl
239 was then added to each well of the Biolog plate. Plates were incubated at 37°C with intermittent
240 shaking for 1 min. during every hour. Optical densities at 595 nm were taken hourly for a total of
241 24 h using a Tecan Sunrise microplate reader and Magellan plate reader software (Tecan
242 Systems Inc., San Jose, CA). Growth characteristics were analyzed by calculating Area under the
243 curve using the Origin 8.5 software. The Area under the curve for the blank well was subtracted
244 from each well to perform the analysis. For growth curves in individual mucus sugars and amino
245 acids, 4 h cultures were pelleted, washed and were diluted 1:40 in M9G (10 mM), M9 D-
246 Gluconate (10 mM), D-Mannose (10 mM), D-Ribose (10 mM), L-Arabinose (10 mM), D-
247 Galactose (10 mM), D-Glucosamine (10 mM), Pyruvic acid (10 mM), D-Trehalose (10 mM),
248 Fructose (10 mM), L-Glutamic acid (5mM), or L-Aspartic acid (30 mM). Mouse intestinal
249 mucus was extracted as described previously (14, 15). Mice gastrointestinal tracts were harvested
250 and then flushed with PBS to remove intestinal contents. Mucus was collected and pooled by
251 gently scraping the surface walls of the intestine using a spatula or blunted blade. The collected
252 mucus was suspended in PBS and vortexed until homogenized. The mucus solution was then

253 centrifuged at 500 x *g* for 10 min and the supernatant collected. Protein concentration was
254 determined using a Bradford assay. Approximately 30 µg/ml of protein was used in M9 medium
255 for experiments involving mucus (14, 51, 52). Each experiment was performed in triplicate with
256 at least two biological replicates. *In vitro* competition assays in mucus and mucus sugars were
257 performed with inoculums prepared as described for *in vivo* competition assays. 100 µl aliquot of
258 the inoculum was added to 5 ml of M9 minimal media supplemented with 10mM of individual
259 mucus sugars or 30 µg/ml of intestinal mucus and grown at 37°C with aeration for 24 h, serially
260 diluted and plated. Competitive index for each assay was calculated as detailed above.

261 **Bioinformatics analysis of OpaR and AphA binding sites**. The consensus binding sequence
262 and position frequency matrix was obtained for OpaR (33) and AphA (53). The position
263 frequency matrix was then used to identify potential binding sites using the MOODS (Motif
264 Occurrence Detection Suite) algorithm (Version 1.0.2.1) (54, 55). The upstream intergenic
265 sequence for the first gene of each operon was obtained from the NCBI database and used to
266 identify putative binding sites. Operon information was obtained from the DOOR2 prokaryotic
267 operon database (56) and was confirmed using the IGV viewer (57) with the RNASeq sequence
268 data. The MOODS tool returned a Log-odds score for each putative binding site that was then
269 used to access probability of binding.

270 **Purification of OpaR**. OpaR was purified using a method previously described (58). Briefly,
271 *opaR* was cloned into the pProEX HTa expression plasmid (Invitrogen) in which an N-terminal
272 6x His tag is fused to *opaR*, separated by a Tobacco Etch Virus (TEV) protease cleavage site.
273 The primer pair SfoIVP2516Fwd/SacIVP2516Rev (**Table S2**) was used to amplify *opaR*
274 (VP2516) from the *V. parahaemolyticus* RIMD2210633 genome using Accura HiFidelity
275 Polymerase (Lucigen, Middleton, WI) following manufacturer's instruction. The *opaR* PCR

276 product was gel cut purified using the Nucleospin Gel and PCR cleanup kit (Macherey-Nagel)
277 and cloned into pJET1.2 using the blunt end ligation protocol. This was transformed into *E. coli*
278 Dh5α using standard $CaCl_2$ transformation protocol. Plasmid DNA was isolated, restriction
279 digested and ligated into pProEX HTa plasmid. The ligation product was transformed into *E. coli*
280 DH5α and plasmid DNA was isolated and confirmed by sequencing before being transformed
281 into *E. coli* BL21(DE3) using standard $CaCl_2$ method. The pProExHtaOpaR plasmid was
282 expressed in *E. coli* BL21(DE3). A volume of 10 mL overnight culture was inoculated into 1 L
283 LB broth at 37°C and induced with 0.5 mM isopropyl-1-thio-β-d-galactopyranoside (IPTG) at
284 OD_{600} 0.5. Growth continued overnight at 18°C. Cells were harvested by centrifugation (5,000 x
285 *g* for 20 min at 4°C) and were re-suspended in immobilized metal affinity chromatography
286 (IMAC) Wash Buffer (50 mM sodium phosphate, 200 mM NaCl, 20 mM imidazole, pH 7.6)
287 supplemented with the protease inhibitors 1 mM phenylmethanesulfonyl fluoride (PMSF) and 1
288 mM benzimidine. Bacterial cells were lysed on ice using a high-pressure homogenizer
289 (EmulsiFlex-C5, Avestin, Ottawa, Canada). Cell debris was removed by centrifugation (15,000 x
290 *g* for 1 h at 4°C). The supernatant was passed through a column containing 5 mL Profinity
291 IMAC resin (Bio-Rad Laboratories, Hercules, CA). The column was washed with 10 column
292 volumes (CV) of IMAC Wash Buffer. The fusion protein, 6xHis-OpaR was eluted with three CV
293 IMAC Elution Buffer (50 mM sodium phosphate, 200 mM NaCl, 500 mM imidazole, pH 7.6). A
294 hexahistidine-tagged TEV protease was added to the eluent in a 1:10 molar ratio (TEV: 6xHis-
295 OpaR) and the cleavage reaction proceeded overnight at 4°C. The cleavage mixture was
296 centrifuged, adjusted to 20 mM imidazole and subject to IMAC using Profinity IMAC resin to
297 remove the His-tagged TEV and any remaining un-cleaved fusion protein. The flow through and
298 one CV of wash with IMAC Wash Buffer contained OpaR. The fractions were combined,

299 concentrated and the buffer exchanged to that of the electrophoretic mobility shifts assays
300 binding buffer (10 mM Tris, 150 mM KCl, 0.1 mM dithiothreitol, 0.1 mM EDTA, 5% PEG, pH
301 7.4). The protein identity was confirmed by mass spectrometry and its purity was determined to
302 be higher than 95% by SDS-PAGE.

303 **Electrophoretic Mobility Shift Assays.** DNA probes VP0008 (amino acid transport), VP1779
304 (putrescine metabolism), VPA1087 (ribose transport), VPA0500 (mannitol PTS transporter),
305 VPA1424 (mannose metabolism) and negative control VPA1667 (glucose-specific PTS
306 transporter), were PCR amplified using Accura HiFidelity Polymerase in 50 µl reactions using
307 corresponding primer sets in **Table S2** with *V. parahaemolyticus* DNA as template. PCR
308 products were separated on a 1% agarose gel and bands excised from the gel were purified using
309 NucleoSpin Gel and PCR clean-up kit (Macherey-Nagel). Purified DNA probes were quantified
310 using a Nanodrop spectrophometer. Varying concentrations of purified OpaR were incubated
311 with 30 ng of target DNA in binding buffer (10 mM Tris, 150 mM KCl, 0.1 mM dithiothreitol,
312 0.1 mM EDTA, 5% PEG, pH 7.4) for 20 min at room temperature and 10 µL were loaded onto a
313 pre-run (200 V for 2 h at 4°C) 6% native acrylamide gel. The gel was run at 200 V for 3 h in 1x
314 Tris-acetate-EDTA (TAE) buffer at 4°C. Following electrophoresis, gels were stained in an
315 ethidium bromide bath (0.5 µg/ml) for 20 min, washed with water and imaged.

316 **Results**

317 **Deletion of *luxO* or *aphA* leads to a defect in intestinal colonization.** To determine the role of
318 the QS regulators in *V. parahaemolyticus* pathogenesis, we examined each of the QS mutants for
319 their ability to colonize the adult mouse intestine. We examined *luxO, aphA* and *opaR* deletion
320 mutant strains as well as double deletion mutants *luxO/opaR* and *opaR/aphA* in *in vivo*
321 competition assays with wild-type using the streptomycin pretreated adult mouse model of

intestinal colonization (13, 14). Mice pretreated with streptomycin were orogastrically co-inoculated with an equal mixture of WBWlacZ (wild-type marked with *lacZ*) and each of the mutants. In these assays, the WBWlacZ strain significantly out-competed the *luxO* mutant, which had a competitive index (CI) of 0.27 indicating that deletion of *luxO* leads to reduced fitness *in vivo* (**Fig. 2**). In order to investigate whether the defect in the *luxO* mutant was through its regulation of the QS regulators AphA or OpaR, we constructed deletion mutants in each of these genes. The *aphA* mutant showed a significant defect in colonization similar to the *luxO* mutant with a CI of 0.39 (Fig 2). Both the *luxO* and *aphA* mutant strains grew similar to wild-type in *in vitro* competition assays in LBS, with CIs of 0.9 and 1.0 respectively. These data show that deletion of *luxO* or *aphA* affects colonization ability specifically (**Fig 2**). The *opaR* mutant behaved similar to the wild-type in both *in vitro* and *in vivo* assays with a CI of ~1. In order to determine further the importance of each of these regulators in colonization, we examined double deletion mutants, *luxO/opaR* and *opaR/aphA*. The deletion of *opaR* in the *luxO* and *aphA* mutant resulted in a significant increase in colonization ability compared to the single *luxO* and *aphA* mutants. Colonization was restored to wild-type levels in the *luxO/opaR* double mutant, which had a CI of 1.4. The *opaR/aphA* mutant also had increased colonization compared to the *aphA* single mutant with a CI of 0.7, however, this mutant still showed a defect in colonization compared to wild-type. (**Fig. 2**). Taken together, these data demonstrate that over-expression of OpaR in the mutant compared to wild type is detrimental and AphA is required for *in vivo* colonization.

The *in vivo* defect observed for the *luxO* mutant is in contrast to the superior colonization phenotype that we had previously showed for an *rpoN* deletion mutant (14). According to the quorum sensing pathway in *V. parahaemolyticus*, deletion of both *luxO* and *rpoN* should have

345 the same effect on the expression of the two master regulators *aphA* and *opaR*. We determined
346 the expression patterns of these regulators in *luxO, opaR, aphA* and *rpoN* mutant strains grown to
347 OD 1.0 in M9G. Expression of *opaR* was significantly induced in the *luxO* mutant with a 6.3-
348 fold change in expression relative to wild-type. The expression of *opaR* was increased in both the
349 *rpoN* and the *aphA* mutants, but not to the same level as in the *luxO* mutant (**Fig. 3A**).
350 Expression of *aphA*, although not significant, was reduced in the *luxO* mutant and was induced
351 in the *opaR* mutant. The expression of *aphA* was not repressed in the *rpoN* mutant (**Fig. 3B**).
352 Both RpoN and its activator LuxO are required for the *qrrs* expression since *qrr1* to *qrr5* each
353 contain a conserved RpoN -12 and -24 promoter binding sequence indicating this sigma factor is
354 involved in expression (35). To address why *aphA* was not repressed and *opaR* is not as highly
355 expressed in the *rpoN* mutant compared to the *luxO* mutant, we examined the expression patterns
356 of *qrr1* to *qrr5* in both these mutants under the same conditions as *opaR* expression. QPCR
357 analysis showed that in the *luxO* mutant compared to wild-type, *qrr2, qrr3* and *qrr5* were
358 repressed, while *qrr1* was unchanged (**Fig. 3C**). In the *rpoN* mutant, qPCR analysis showed that
359 *qrr1, qrr3* and *qrr5* were repressed, however *qrr2* was not repressed compared to wild-type (**Fig.**
360 **3D**). In both cases, *qrr4* expression was either very low or altogether not detected. The most
361 notable difference in expression patterns between the *luxO* and *rpoN* mutants was in *qrr2*. While
362 *qrr2* was significantly downregulated in the *luxO* mutant, its expression was not repressed in the
363 *rpoN* mutant. We speculate that the differential expression of *qrr2* in the *rpoN* mutant may
364 explain the reduced level of *opaR* compared to the *luxO* mutant.

365 The *V. parahaemolyticus* quorum sensing master regulators OpaR and AphA have been
366 shown to regulate CPS production and biofilm formation (25, 30, 41, 59, 60). We examined
367 these phenotypes in the QS regulator mutants examined in this study. The *luxO* and *aphA*

368 mutants produced rugose colonies similar to wild-type indicating CPS production, which
369 indicates that CPS production is not involved in the *in vivo* phenotype of these mutants (**Fig.**
370 **S1A**). The *luxO* and *aphA* mutants produced similar amount of biofilm as wild-type at the initial
371 time points but were found to be defective at 24 h (**Fig S1B**). Previously, we showed that an
372 *rpoN* mutant had a defective in biofilm formation but had a superior colonization phenotype
373 suggesting this is not the cause of the *luxO* and *aphA* mutants *in vivo* phenotypes.

374 **RNA-seq data and comparative analysis of gene expression in mouse intestinal mucus.** To
375 begin to determine the mechanism of the *in vivo luxO* mutant colonization defect, we performed
376 RNA-Seq expression analysis of the wild-type and the *luxO* mutant strains. RNA was isolated
377 from both strains grown to early exponential phase in M9 supplemented with mouse intestinal
378 mucus as the sole carbon source. The LCD time point was chosen since it should show
379 maximum differences in *opaR* expression between the wild-type (low OpaR levels) and the *luxO*
380 mutant (high OpaR levels). Sequencing resulted in greater than 10 million sequence reads
381 obtained for each sample (**Fig. S2A**). Over 98% of the reads aligned to genomic features
382 including mRNA, tRNA, sRNA or to unannotated regions of the genome. The rRNA depletion
383 procedure resulted in less than 0.5% of the reads aligning to these features in the genome (**Fig.**
384 **S2A and S2B**). Differential expression analysis revealed that 106 genomic features and 102
385 features were downregulated and upregulated (> 2-fold, $P_{adj} < 1x10^{-4}$) respectively in the *luxO*
386 mutant compared to wild-type (**Fig. S3**, **Table S3 and S4**). Of the total 208 differentially
387 regulated features, 134 were from chromosome I and 74 were from chromosome II (**Table S3**
388 **and S4**). The 106 downregulated features were all annotated ORFs. The 102 upregulated
389 features included 93 annotated ORFs, 3 small RNAs and 6 tRNAs. The *opaR* gene was induced
390 and *aphA* was repressed in the *luxO* mutant compared to wild-type and this was confirmed by

391 qPCR (**Fig. 4A**). Expression analysis of the ***qrrs*** by qPCR showed that *qrr5* was significantly
392 downregulated in the *luxO* mutant (**Fig. 4A**). Twenty-one of the genes upregulated in the *luxO*
393 mutant belonged to the T6SS-2 region on chromosome II (VPA1024 - 44), which was previously
394 shown to be positively regulated by OpaR (30). QPCR analysis of VPA1027 (*hcp2*) from the
395 T6SS-2 cluster confirmed that in the *luxO* mutant this gene was induced (**Fig. 4C**). Furthermore,
396 qPCR analysis of *hcp1* (VP1393) from the T6SS-1 cluster and *yopD* (VP1656) from the T3SS-1
397 cluster showed their expression was reduced compared to wild-type (**Fig. 4C**). The most highly
398 upregulated genes in the *luxO* mutant were genes for the replication and synthesis of the
399 filamentous phage f237 (VP1550-VP1562). Many genes within the class-1 integron region on
400 chromosome I (VP1790-VP1851) were also induced in the *luxO* mutant compared to wild-type
401 (Table S3A). The majority of the genes within the f237 phage and the class-1 integron were
402 categorized into the COG classes S: Function unknown and R: General function prediction only
403 (**Fig. S4A**). The T6SS-2 genes were classified into the COG class U: Intracellular trafficking,
404 secretion and vesicular transport (**Fig. S4A**). Among the downregulated COG classes, most
405 interesting to note was that 60% of the genes were classified into categories involved in
406 metabolism and transport (**Fig. S4B**).

407 **Metabolism and transporter genes are downregulated in the *luxO* mutant.** Of the 106
408 genomic features downregulated in the *luxO* mutant, 64 genes were involved in transport and
409 metabolism of amino acids, carbohydrate and lipids (**Fig S4B and Table S4**). Downregulated
410 gene clusters that comprised amino acid transport and metabolism included arginine biosynthesis
411 (VP2756-VP2760) and transport (VPA0637-VPA0639) (Fig S4A), phenylalanine/ tyrosine
412 biosynthesis (VP0546-VP0547, VP0555) and histidine biosynthesis (VP1137-VP1138). QPCR
413 analysis confirmed the downregulation of VP2756 (*argH*), an ORF in the arginine biosynthesis

414 (VP2756-VP2760) pathway (**Fig. 4B**). The carbohydrate metabolism and transport genes
415 downregulated in the *luxO* mutant included genes involved in D-mannitol metabolism
416 (VPA0501-0502), D-galactose degradation (VP2397-VP2400) and L-arabinose transport and
417 metabolism (VPA1671-VP1677) (**Table S4**). QPCR analysis confirmed the downregulation of
418 VPA1674 (*araB*), an ORF in the arabinose catabolism pathway (**Fig. 4B**). A region required for
419 tetrathionate reductase synthesis (VP2012-VP2016) was also repressed in the *luxO* mutant
420 compared to wild-type. Tetrathionate can be used as an electron donor that is produced in
421 vertebrate intestinal mucosa from thiosulphate by the action of tetrathionate reductase (61).
422 VP1771-VP1779 and VP1781-VP1782 are two operons involved in the polyamine putrescine
423 utilization and all ORFs within this region were downregulated in the *luxO* mutant, which was
424 confirmed by qPCR analysis of VP1779 (*puuD*) (**Fig. 4B**). ORFs VP1447 to VP1451 are
425 homologs of genes required for the synthesis of a putative anaerobic dimethyl sulfoxide
426 reductase and these genes were all downregulated in the *luxO* mutant. There were eight putative
427 transcription regulators downregulated in the *luxO* mutant compared to wild-type, VP0358
428 (DeoR), VP1778 (PuuR), VP3009 (AraC/XylS family), VPA0053 (TetR family), VPA0251
429 (LysR family), VPA0717 (LysR family), VPA0883 (LysR family), and VPA1678 (AraC/XylS
430 family). In addition, genes for compatible solute biosynthesis were also downregulated, two
431 genes in the ectoine biosynthesis pathway (VP1721-VP1720) and two genes involved in betaine
432 biosynthesis (VPA1112) and transport (VPA1111) operon (**Table S4**).

433 **Growth comparisons of wild-type and mutant strains on different carbon sources.** Our
434 RNA-seq data suggests that *luxO* could be at a metabolic disadvantage given the down regulation
435 of many metabolism and transporter genes. Thus, the growth patterns of the wild-type and QS
436 mutants were examined in 190 carbon sources to determine whether there were differences

437 among the strains. A total of 71 different carbon sources were utilized by wild-type *V.*
438 *parahaemolyticus* (**Fig. S5**). There was a total of 33 substrates that the *luxO* mutant showed a
439 defect in compared to the wild-type, seven substrates of which showed a defect only in the *luxO*
440 mutant. The *aphA* mutant showed a significant defect in 30 substrates, five of which were unique
441 to the mutant while 13 carbon sources showed defects also in the *luxO* (**Fig. S5**). Thus, there
442 were 25 carbon substrates that the *luxO* and *aphA* mutants showed a growth defect whereas the
443 *opaR* mutant did not show a defect in these substrates. These 25 carbon sources included 6
444 amino acids or their derivatives, 4 dipeptides, 7 sugars, 2 nucleosides, 1 TCA cycle metabolite
445 and 5 miscellaneous carbon sources (**Fig. S5**). The most significant growth defects in the *luxO*
446 mutant were growth on amino acids and their dipeptide derivatives; L-Aspartic acid, Glycyl-L-
447 Aspartic acid, Glycyl-L-Glutamic, Glycyl L- Proline acid, L-Serine and L-Threonine (**Fig. S5**).
448 The *luxO* and *aphA* mutants also showed notable defects in L-Glutamic acid and L-Arginine, 2
449 TCA cycle metabolites (Pyruvic acid and α-Keto-Glutaric acid) and 2 polysaccharides (Glycogen
450 and inulin). We confirmed many of these growth defects by examining the growth pattern of the
451 QS mutants in 12 of the carbon sources (**Fig. S6**). The *opaR* mutant did not show a defect in
452 these carbon sources and grew similar to wild-type (**Fig. S6**). These data suggest that the QS
453 regulators may play a key role in regulation of cell metabolism. In addition, considering many of
454 these carbon sources are components of intestinal mucus, which is the primary carbon source
455 available for the bacteria *in vivo*, this disadvantage could contribute to these mutants being out-
456 competed by the wild-type *in vivo*.

457 **Deletion of *opaR* leads to increased metabolic fitness in intestinal mucus and its**
458 **components.** Intestinal mucus is composed of glycoproteins known as mucins that are
459 comprised of 80% oligosaccharide and 20% protein. The main sugars in mucin include fucose,

galactose, mannose, sialic acid, N-acetyl glucosamine, and N-acetyl galactosamine, as well as arabinose, ribose, gluconate, galacturonate, and glucoronate. The three main amino acids that make up the protein core of mucin are serine, threonine and proline (62-66). From genomic analysis, we known that *V. parahaemolyticus* cannot utilize fucose, sialic acid, or galacturonate, and only clinical strains can utilize arabinose. We examined growth of the *luxO, aphA* and *opaR* mutants on M9 supplemented individual mucus sugars as the sole carbon source (**Fig. S6**). These data demonstrate that the *luxO* and *aphA* mutants had significantly longer lag phases than wild-type when grown on these substrates. These longer lag phases indicate that these mutants would be at a significant disadvantage at utilizing mucus as a carbon source in comparison to the wild-type strain.

In order to assess whether the metabolic fitness effects could account for the defect of the *luxO* and *aphA* mutant *in vivo*, we performed *in vitro* competition assays in M9 supplemented with mucus (M9M) or M9 with individual mucus sugars as sole carbon sources (**Fig. 5**). We observed that the *luxO* mutant was out-competed in intestinal mucus with a CI of 0.6 (**Fig. 5**) and mucus sugars gluconate, ribose and arabinose with a CI of 0.3, 0.24 and 0.25 (**Fig. 5)**. The *aphA* mutant was also significantly out-competed by the wild-type in intestinal mucus with a CI of 0.59 and mucus sugars ribose and arabinose with a CI of 0.67 and 0.66 respectively (**Fig. 5**). In addition, the competitive indices for the *opaR* mutant in *in vitro* competition assays showed the mutant significantly out-competed the wild-type in intestinal mucus with a CI of 1.6 (**Fig. 5**). The *opaR* mutant also significantly out-competed wild-type in individual mucus sugars; mannose, ribose and arabinose with a CI of 1.6, 1.6 and 1.5 respectively (**Fig. 5**). Overall, the *in vitro* metabolic assays suggest that not only is the presence of *aphA* important to the cells, in part due to its regulation of *opaR,* but also induced expression of *opaR* can have a detrimental effect.

While constitutive expression of *opaR* results in a fitness defect (*luxO* mutant), deletion of *opaR* provides a fitness advantage (*opaR* mutant) *in vitro*.

OpaR binding sites in the promoter regions of carbon transport and metabolism genes. Both the *luxO* and *aphA* mutants have a constitutively expressed *opaR* and a repressed *aphA*. We wanted to determine whether the observed *in vitro* growth phenotypes were due to direct or indirect regulation of metabolism and transporter genes by OpaR. First, we performed bioinformatics analysis to identify putative binding sites for OpaR in the promoter regions of 89 metabolism and transporter genes. We choose genes that were involved in the transport and metabolism of carbon sources that showed different growth patterns between wild-type and mutants in the phenotypic arrays. The MOODS tool was used to identify OpaR and AphA binding sites using the consensus sequence and position frequency matrix identified by Zhang et al (33) and Sun et al (53). In this analysis, we identified 55 promoter regions with strong binding sites ($P <= 0.005$ and >90% probability) for OpaR (**Table S5**). Interestingly the same analysis for AphA consensus binding sequence only identified 9 putative AphA binding sites suggesting that OpaR is the main QS regulator of metabolism (**Table S5**). Of the 55 putative OpaR binding sites, 28 OpaR binding sites were in promoter regions of operons and 27 binding sites were in single gene promoter regions. These included genes for arabinose, ribose, glucose, maltose, trehalose, mannitol, mannose, glycogen, glycerol, cellobiose and sperimidine/putrescine transport and/or metabolism. Putative OpaR binding sites were identified also in genes for a general amino acid transport (ORFs VP0008-VP0006, VP1620), thymidine, urdine, serine, aspartate, fumarate, glutarate, arginine, histidine, phenylalanine, tyrosine and tryptophan transport and/or metabolism. In contrast, of the 89 promoter regions examined for AphA binding sites only 9 promoter regions showed strong binding sites (probability >90%), which included

506 mannose (VPA1424-VPA1425), arabinose (VPA1673-VPA1671), and glycogen (VPA1620)
507 transport and/or metabolism genes (**Table S6**).

508 In order to validate the bioinformatics analysis of putative OpaR binding sites, we
509 purified OpaR to homogeneity and performed EMSAs on five representative target promoter
510 regions. The five targets were comprised of an amino acid transporter promoter region VP0008-
511 VP0006, the polyamine putrescine cluster VP1779-VP1771, two sugar transporter promoter
512 regions, mannitol (VPA0500-VPA0501) and ribose (VPA1087-VPA1084) and a promoter region
513 for mannose transport and metabolism cluster (VPA1424-VPA1425). The glucose-specific PTS
514 VPA1667 probe, was included as a negative control as it did not have any predicted OpaR
515 binding sites. (**Fig. 6**). For the P*VP0008*, OpaR bound to the 323-bp DNA probe with increasing
516 concentration of OpaR protein (0-2.7 μM). Similarly, promoter regions P*VP1779* (244-bp),
517 P*VPA1087* (333-bp), P*VPA0500* (360-bp) and P*VPA1424* (350-bp) were bound by OpaR in a
518 concentration dependent manner (**Fig. 6**). The negative DNA control target remained unbound
519 by OpaR at the highest concentrations tested (**Fig. 6**). These data demonstrate that OpaR binding
520 is specific and that OpaR regulates the expression of these targets indicating that it plays a direct
521 role in cell metabolism.

522 **Discussion**

523 In this study, we examined the role of QS regulators in *V. parahaemolyticus*
524 pathogenesis, specifically their role in intestinal colonization. The *in vivo* colonization data show
525 that the QS regulators are essential for efficient colonization. RNA-Seq transcriptome data
526 between the *luxO* mutant and wild-type cells showed global gene expression differences. A
527 striking feature of this data is the number of genes involved in cell metabolism and transport that

528 were downregulated in the *luxO* mutant compared to wild-type. These included genes required
529 for transport and metabolism of substrates present in intestinal mucus, one of the main nutrient
530 source *in vivo*. The gene expression data suggested that the *luxO* mutant could have metabolic
531 defects based on the down regulation of key metabolism genes. Competition for intestinal
532 nutrients and the ability to utilize intestinal mucus as a carbon and energy source has been shown
533 to be important for successful colonization of intestinal bacteria (67-70). Phenotypic array data
534 showed that the deletion of *luxO* resulted in metabolic defects, with the mutant demonstrating a
535 defect in growth on a number of carbon sources. This was also showed to be the case for the
536 *aphA* mutant, which showed a growth defect compared to wild-type in 25 carbon sources. The
537 carbon substrates in which the mutants showed defects were comprised of nearly equal number
538 of sugars, organic acids and peptides indicating that not just one pathway was affected. Some of
539 the most significant growth defects were in the utilization of amino acids and amino acid
540 derivatives, key intermediates in central metabolism. The *luxO* mutant also had a defect in *in*
541 *vitro* competition assays in mucus. This is not too surprising given that mucus is made of mainly
542 the glycoprotein mucin and is therefore rich in amino acids as well as sugars (63-66). Neither the
543 *aphA* nor the *opaR* mutants demonstrated a dramatic *in vitro* metabolic fitness effects compared
544 to the *luxO* mutant although each had slightly different growth patterns in one or two carbon
545 sources. One scenario to explain these differences is that in the *luxO* mutant, *aphA* expression is
546 down as is *qrr* expression and *opaR* expression is highly induced. In the *aphA* mutant, *opaR* is
547 induced, but so too should be the *qrrs*, which are negatively regulated by AphA in *V. harveyi*.
548 Thus knocking out both *aphA* and *qrr* expression is more detrimental than just knocking out
549 *aphA* alone. This suggests that there may be dual regulation of genes involved in metabolism
550 and/or additional roles for the Qrrs.

551 A transcriptome study of *Pseudomonas aeruginosa* over 10 years ago demonstrated that
552 the QS activated regulon was over represented by genes involved in intermediate central
553 metabolism (71). They showed that the QS repressed regulon showed carbohydrate utilization
554 and nutrient transport genes were the most abundant representatives (71). A more recent study in
555 the same species demonstrated a global impact of QS on the metabolome and proposed that QS
556 plays a key role in metabolic rewiring of the cell under certain conditions (72). A study
557 examining the targets of LuxR homologues in *Brucella* an intracellular pathogen, identified a
558 large number of proteins involved in metabolic pathways such as central metabolism or amino
559 acid metabolism, respiration, transport of amino acids and sugars that were under the control of
560 QS regulators (73). QS control of metabolic pathways that affects fitness has also been shown in
561 *Burkholderia* species (74). Hwang and colleagues showed that QS regulates oxalate synthesis to
562 counteract alkalization of the growth medium and was essential for fitness (74, 75). More
563 recently this same group has demonstrated that the QS master regulator QsmR down regulates
564 glucose transport, substrate-level and oxidative phosphorylation and nucleotide biosynthesis
565 acting as a metabolic brake on individuals as the population increases (75). Evidence for a role
566 for LuxR in metabolism also comes from *Vibrio* species. In *V. harveyi*, it was demonstrated that
567 the *argA, purM, lysE, and rluA* promoter regions were LuxR dependent, genes involved in
568 arginine and purine biosynthesis, amino acid efflux, and pseudouridine synthesis, respectively
569 (76). In addition, it was demonstrated in *V. fischeri* that QS AinS signaling is essential for
570 control of the acetate switch and this regulation is mediated through the LuxR homolog LitR
571 (77). A recent study in *V. cholerae* showed that the QS LuxR homolog HapR regulated chitin
572 metabolism that provided predator grazing resistance in biofilms. They showed that 19 of 22

genes involved in GlcNAc catabolism were repressed in a *hapR* mutant compared to wild-type (78).

QS regulators are required for both population level and individual control of gene expression, which corresponds to stationary phase and early exponential growth phases respectively, during which availability of the type and amount of nutrients is very different. Thus, the involvement of QS regulators controlling expression of transporter and metabolism genes makes biological sense. The *luxO* and *aphA* mutants had an *in vivo* defect that correlates to reduced metabolic fitness. In both these mutants OpaR is highly expressed, which suggests that OpaR could be a direct or indirect negative regulator of cell metabolism. Our RNA-seq data revealed that in the *luxO* mutant 60% of downregulated were involved in transport and metabolism. In addition, in the *luxO* mutant a number of regulators that could be involved in regulation of metabolism were also downregulated. These included genes belonging to the LysR family of proteins, which have been shown to regulate a diverse set of genes including those involved in metabolism (79), the AraC/XylS family of transcriptional regulators, which are predominantly involved in the regulation of carbon metabolism (80). Interestingly, we also found that the DNA-binding protein Fis (VP2885) was slightly upregulated in the *luxO* mutant (1.62-fold, Padj < 0.0001). Fis is a known global regulator of metabolism. In *Salmonella enterica*, Fis was shown to negatively regulate genes contributing to metabolism in the mammalian gut (81). In addition, the Hfq-binding sRNA Spot 42 was upregulated in the *V. parahaemolyticus luxO* mutant. In *E. coli*, Spot 42 plays an essential role as a regulator in carbohydrate metabolism and uptake, and its expression is activated by glucose and inhibited by CRP. Spot 42 was shown to be a negative regulator of metabolism of many sugars in both *E. coli* and *Vibrio* (*Allivibrio) salmonicida* (82-85). A second sRNA, VrrA was also induced in the *V. parahaemolyticus luxO*

596 mutant. In *V. cholerae,* studies showed that a *vrrA* mutant had a 5-fold increased ability to
597 colonize infant mice (86). VrrA downregulates outer membrane proteins, OmpA and OmpT, the
598 stationary phase survival factor Vrp and biofilm matrix protein RbmC in *V. cholerae* (87, 88).

599 To determine the possible extent of direct regulation of cell metabolism and transport by
600 the QS regulators we performed bioinformatics analysis and examined 89 regulatory regions of
601 metabolism genes for the presence of putative OpaR and AphA binding sites. We identified 55
602 loci that contained strong putative OpaR binding sites and only 9 AphA putative binding sites.
603 From the 55 loci with putative OpaR binding sites, we chose five representatives to examine
604 further using EMSAs; a general amino acid transporter (VP0008-VP0006), ribose (VPA1087-
605 VPA1084) and mannose (VPA1424-VPA1425) metabolism and transporter, mannitol
606 (VPA0500-VPA0501) and putrescine metabolism (VP1771-VP1779) regulatory regions. We
607 investigated the regulatory region of the general amino acid transporter since both microarray
608 and RNA-seq analysis showed repression of these genes by OpaR (30, 42). Our binding analysis
609 confirmed that indeed OpaR does bind to the regulatory region of this operon. We examined the
610 ribose and mannose regulatory regions since these sugars are important mucus sugars and we
611 observed growth defects in these sugars in the *luxO* and *aphA* mutants compared to wild-type.
612 We investigated binding to the regulatory region of the transporter of sugar alcohol mannitol
613 because it had one of the strongest putative OpaR binding sites. The polyamine putrescine cluster
614 VP1779-VP1771 is involved in putrescine metabolism and contains genes that shuttle into
615 multiple metabolic pathways. All the genes in this pathway were downregulated in the *luxO*
616 mutant compared to wild-type, and this was confirmed by qPCR and EMSA analysis showed
617 binding of OpaR to the regulatory region. These data indicate that OpaR is a negative regulator
618 of putrescine metabolism. Thus, EMSA analysis demonstrated binding to all five regulatory

regions and no binding to the negative control using the highest concentration of OpaR. These data demonstrate a direct role for OpaR in cell metabolism and suggest that this role may be more prevalent than previously appreciated.

ACKNOWLEDGEMENTS

We thank Nathan McDonald, Abish Regmi, Joe Borowski, Gwen Gregory and Aoife Boyd for reviewing the manuscript and helpful discussions. This work was supported in part by a National Science Foundation grant DEB-0844409 to EFB and departmental funds.

REFERENCES

1. **Hondo S, Goto I, Minematsu I, Ikeda N, Asano N, Ishibashi M, Kinoshita Y, Nishibuchi N, Honda T, Miwatani T.** 1987. Gastroenteritis due to Kanagawa negative *Vibrio parahaemolyticus*. Lancet **1:**331-332.
2. **Daniels NA, MacKinnon L, Bishop R, Altekruse S, Ray B, Hammond RM, Thompson S, Wilson S, Bean NH, Griffin PM, Slutsker L.** 2000. *Vibrio parahaemolyticus* infections in the United States, 1973-1998. J. Infect. Dis. **181:**1661-1666.
3. **McLaughlin JB, DePaola A, Bopp CA, Martinek KA, Napolilli NP, Allison CG, Murray SL, Thompson EC, Bird MM, Middaugh JP.** 2005. Outbreak of *Vibrio parahaemolyticus* gastroenteritis associated with Alaskan oysters. N Engl J Med **353:**1463-1470.
4. **Nair GB, Ramamurthy T, Bhattacharya SK, Dutta B, Takeda Y, Sack DA.** 2007. Global dissemination of *Vibrio parahaemolyticus* serotype O3:K6 and its serovariants. Clin Microbiol Rev **20:**39-48.
5. **Qadri F, Alam MS, Nishibuchi M, Rahman T, Alam NH, Chisti J, Kondo S, Sugiyama J, Bhuiyan NA, Mathan MM, Sack DA, Nair GB.** 2003. Adaptive and inflammatory immune responses in patients infected with strains of *Vibrio parahaemolyticus*. J Infect Dis **187:**1085-1096.
6. **Makino K, Oshima K, Kurokawa K, Yokoyama K, Uda T, Tagomori K, Iijima Y, Najima M, Nakano M, Yamashita A, Kubota Y, Kimura S, Yasunaga T, Honda T, Shinagawa H, Hattori M, Iida T.** 2003. Genome sequence of *Vibrio parahaemolyticus*: a pathogenic mechanism distinct from that of *V cholerae*. Lancet **361:**743-749.
7. **Ham H, Orth K.** 2012. The role of type III secretion system 2 in *Vibrio parahaemolyticus* pathogenicity. J Microbiol **50:**719-725.

8. **O'Boyle N, Boyd A.** 2014. Manipulation of intestinal epithelial cell function by the cell contact-dependent type III secretion systems of *Vibrio parahaemolyticus*. Front Cell Infect Microbiol **3:**114.
9. **Hiyoshi H, Kodama T, Iida T, Honda T.** 2010. Contribution of *Vibrio parahaemolyticus* virulence factors to cytotoxicity, enterotoxicity, and lethality in mice. Infect Immun **78:**1772-1780.
10. **Park KS, Ono T, Rokuda M, Jang MH, Okada K, Iida T, Honda T.** 2004. Functional characterization of two type III secretion systems of *Vibrio parahaemolyticus*. Infect Immun **72:**6659-6665.
11. **Pineyro P, Zhou X, Orfe LH, Friel PJ, Lahmers K, Call DR.** 2010. Development of two animal models to study the function of *Vibrio parahaemolyticus* type III secretion systems. Infect Immun **78:**4551-4559.
12. **Ritchie JM, Rui H, Zhou X, Iida T, Kodoma T, Ito S, Davis BM, Bronson RT, Waldor MK.** 2012. Inflammation and disintegration of intestinal villi in an experimental model for *Vibrio parahaemolyticus*-induced diarrhea. PLoS Pathog **8:**e1002593.
13. **Whitaker WB, Parent MA, Boyd A, Richards GP, Boyd EF.** 2012. The *Vibrio parahaemolyticus* ToxRS regulator is required for stress tolerance and colonization in a novel orogastric streptomycin-induced adult murine model. Infect Immun **80:**1834-1845.
14. **Whitaker WB, Richards GP, Boyd EF.** 2014. Loss of Sigma Factor RpoN Increases Intestinal Colonization of *Vibrio parahaemolyticus* in an Adult Mouse Model. Infect Immun **82:**544-556.
15. **Haines-Menges B, Whitaker WB, Boyd EF.** 2014. Alternative sigma factor RpoE is important for *Vibrio parahaemolyticus* cell envelope stress response and intestinal colonization. Infect Immun **82:**3667-3677.
16. **Hubbard TP, Chao MC, Abel S, Blondel CJ, Abel Zur Wiesch P, Zhou X, Davis BM, Waldor MK.** 2016. Genetic analysis of *Vibrio parahaemolyticus* intestinal colonization. Proc Natl Acad Sci U S A **113:**6283-6288.
17. **Fuqua WC, Winans SC, Greenberg EP.** 1994. Quorum sensing in bacteria: the LuxR-LuxI family of cell density-responsive transcriptional regulators. J Bacteriol **176:**269-275.
18. **Hardman AM, Stewart GS, Williams P.** 1998. Quorum sensing and the cell-cell communication dependent regulation of gene expression in pathogenic and non-pathogenic bacteria. Antonie Van Leeuwenhoek **74:**199-210.
19. **Hastings JW, Nealson KH.** 1977. Bacterial bioluminescence. Annu Rev Microbiol **31:**549-595.
20. **Bassler BL.** 1999. How bacteria talk to each other: regulation of gene expression by quorum sensing. Curr Opin Microbiol **2:**582-587.
21. **Bassler BL, Wright M, Showalter RE, Silverman MR.** 1993. Intercellular signalling in *Vibrio harveyi*: sequence and function of genes regulating expression of luminescence. Mol Microbiol **9:**773-786.
22. **Ng WL, Bassler BL.** 2009. Bacterial quorum-sensing network architectures. Annu Rev Genet **43:**197-222.
23. **Miyamoto CM, Dunlap PV, Ruby EG, Meighen EA.** 2003. LuxO controls *luxR* expression in *Vibrio harveyi*: evidence for a common regulatory mechanism in *Vibrio*. Mol Microbiol **48:**537-548.

24. **Gray KM, Passador L, Iglewski BH, Greenberg EP.** 1994. Interchangeability and specificity of components from the quorum-sensing regulatory systems of Vibrio fischeri and Pseudomonas aeruginosa. J Bacteriol **176:**3076-3080.
25. **McCarter LL.** 1998. OpaR, a homolog of *Vibrio harveyi* LuxR, controls opacity of *Vibrio parahaemolyticus*. J Bacteriol **180:**3166-3173.
26. **Miller MB, Skorupski K, Lenz DH, Taylor RK, Bassler BL.** 2002. Parallel quorum sensing systems converge to regulate virulence in *Vibrio cholerae*. Cell **110:**303-314.
27. **Jaques S, McCarter LL.** 2006. Three new regulators of swarming in *Vibrio parahaemolyticus*. J Bacteriol **188:**2625-2635.
28. **Milton DL.** 2006. Quorum sensing in vibrios: complexity for diversification. Int J Med Microbiol **296:**61-71.
29. **Hammer BK, Bassler BL.** 2003. Quorum sensing controls biofilm formation in *Vibrio cholerae*. Mol Microbiol **50:**101-104.
30. **Gode-Potratz CJ, McCarter LL.** 2011. Quorum sensing and silencing in *Vibrio parahaemolyticus*. J Bacteriol **193:**4224-4237.
31. **Henke JM, Bassler BL.** 2004. Quorum sensing regulates type III secretion in *Vibrio harveyi* and *Vibrio parahaemolyticus*. J Bacteriol **186:**3794-3805.
32. **Wang L, Zhou D, Mao P, Zhang Y, Hou J, Hu Y, Li J, Hou S, Yang R, Wang R, Qiu J.** 2013. Cell density- and quorum sensing-dependent expression of type VI secretion system 2 in *Vibrio parahaemolyticus*. PLoS One **8:**e73363.
33. **Zhang Y, Qiu Y, Tan Y, Guo Z, Yang R, Zhou D.** 2012. Transcriptional regulation of opaR, qrr2-4 and aphA by the master quorum-sensing regulator OpaR in *Vibrio parahaemolyticus*. PLoS One **7:**e34622.
34. **Zhou D, Yan X, Qu F, Wang L, Zhang Y, Hou J, Hu Y, Li J, Xin S, Qiu J, Yang R, Mao P.** 2013. Quorum sensing modulates transcription of cpsQ-mfpABC and mfpABC in *Vibrio parahaemolyticus*. Int J Food Microbiol **166:**458-463.
35. **Lilley BN, Bassler BL.** 2000. Regulation of quorum sensing in *Vibrio harveyi* by LuxO and sigma-54. Mol Microbiol **36:**940-954.
36. **Tu KC, Bassler BL.** 2007. Multiple small RNAs act additively to integrate sensory information and control quorum sensing in *Vibrio harveyi*. Genes Dev **21:**221-233.
37. **Lenz DH, Mok KC, Lilley BN, Kulkarni RV, Wingreen NS, Bassler BL.** 2004. The small RNA chaperone Hfq and multiple small RNAs control quorum sensing in *Vibrio harveyi* and *Vibrio cholerae*. Cell **118:**69-82.
38. **Bardill JP, Zhao X, Hammer BK.** 2011. The *Vibrio cholerae* quorum sensing response is mediated by Hfq-dependent sRNA/mRNA base pairing interactions. Mol Microbiol **80:**1381-1394.
39. **van Kessel JC, Rutherford ST, Shao Y, Utria AF, Bassler BL.** 2013. Individual and combined roles of the master regulators AphA and LuxR in control of the *Vibrio harveyi* quorum-sensing regulon. J Bacteriol **195:**436-443.
40. **Rutherford ST, van Kessel JC, Shao Y, Bassler BL.** 2011. AphA and LuxR/HapR reciprocally control quorum sensing in vibrios. Genes Dev **25:**397-408.
41. **Wang L, Ling Y, Jiang H, Qiu Y, Qiu J, Chen H, Yang R, Zhou D.** 2013. AphA is required for biofilm formation, motility, and virulence in pandemic *Vibrio parahaemolyticus*. Int J Food Microbiol **160:**245-251.

42. **Kernell Burke A, Guthrie LT, Modise T, Cormier G, Jensen RV, McCarter LL, Stevens AM.** 2015. OpaR controls a network of downstream transcription factors in *Vibrio parahaemolyticus* BB22OP. PLoS One **10:**e0121863.
43. **Salomon D, Klimko JA, Orth K.** 2014. H-NS regulates the *Vibrio parahaemolyticus* type VI secretion system 1. Microbiology **160:**1867-1873.
44. **Gu D, Liu H, Yang Z, Zhang Y, Wang Q.** 2016. Chromatin Immunoprecipitation Sequencing Technology Reveals Global Regulatory Roles of Low-Cell-Density Quorum-Sensing Regulator AphA in the Pathogen Vibrio alginolyticus. J Bacteriol **198:**2985-2999.
45. **Skorupski K, Taylor RK.** 1999. A new level in the *Vibrio cholerae* ToxR virulence cascade: AphA is required for transcriptional activation of the tcpPH operon. Mol Microbiol **31:**763-771.
46. **Yang M, Frey EM, Liu Z, Bishar R, Zhu J.** 2010. The virulence transcriptional activator AphA enhances biofilm formation by *Vibrio cholerae* by activating expression of the biofilm regulator VpsT. Infect Immun **78:**697-703.
47. **Whitaker WB, Parent MA, Naughton LM, Richards GP, Blumerman SL, Boyd EF.** 2010. Modulation of responses of *Vibrio parahaemolyticus* O3:K6 to pH and temperature stresses by growth at different salt concentrations. Appl Environ Microbiol **76:**4720-4729.
48. **Horton RM, Hunt HD, Ho SN, Pullen JK, Pease LR.** 1989. Engineering hybrid genes without the use of restriction enzymes: gene splicing by overlap extension. Gene **77:**61-68.
49. **Kalburge SS, Whitaker WB, Boyd EF.** 2014. High-salt preadaptation of *Vibrio parahaemolyticus* enhances survival in response to lethal environmental stresses. J Food Prot **77:**246-253.
50. **Pfaffl MW.** 2001. A new mathematical model for relative quantification in real-time RT-PCR. Nucleic Acids Res **29:**e45.
51. **Cohen PS, Laux DC.** 1995. Bacterial adhesion to and penetration of intestinal mucus in vitro. Methods Enzymol **253:**309-314.
52. **Leatham MP, Stevenson SJ, Gauger EJ, Krogfelt KA, Lins JJ, Haddock TL, Autieri SM, Conway T, Cohen PS.** 2005. Mouse intestine selects nonmotile flhDC mutants of Escherichia coli MG1655 with increased colonizing ability and better utilization of carbon sources. Infect Immun **73:**8039-8049.
53. **Sun F, Zhang Y, Wang L, Yan X, Tan Y, Guo Z, Qiu J, Yang R, Xia P, Zhou D.** 2012. Molecular characterization of direct target genes and cis-acting consensus recognized by quorum-sensing regulator AphA in *Vibrio parahaemolyticus*. PLoS One **7:**e44210.
54. **Korhonen J, Martinmaki P, Pizzi C, Rastas P, Ukkonen E.** 2009. MOODS: fast search for position weight matrix matches in DNA sequences. Bioinformatics **25:**3181-3182.
55. **Pizzi C, Rastas P, Ukkonen E.** 2011. Finding significant matches of position weight matrices in linear time. IEEE/ACM Trans Comput Biol Bioinform **8:**69-79.
56. **Mao F, Dam P, Chou J, Olman V, Xu Y.** 2009. DOOR: a database for prokaryotic operons. Nucleic Acids Res **37:**D459-463.

57. **Thorvaldsdottir H, Robinson JT, Mesirov JP.** 2013. Integrative Genomics Viewer (IGV): high-performance genomics data visualization and exploration. Brief Bioinform **14:**178-192.

58. **Carpenter MR, Rozovsky S, Boyd EF.** 2015. Pathogenicity Island Cross Talk Mediated by Recombination Directionality Factors Facilitates Excision from the Chromosome. J Bacteriol **198:**766-776.

59. **Enos-Berlage JL, Guvener ZT, Keenan CE, McCarter LL.** 2005. Genetic determinants of biofilm development of opaque and translucent *Vibrio parahaemolyticus*. Mol Microbiol **55:**1160-1182.

60. **Guvener ZT, McCarter LL.** 2003. Multiple regulators control capsular polysaccharide production in *Vibrio parahaemolyticus*. J Bacteriol **185:**5431-5441.

61. **Liu YW, Denkmann K, Kosciow K, Dahl C, Kelly DJ.** 2013. Tetrathionate stimulated growth of Campylobacter jejuni identifies a new type of bi-functional tetrathionate reductase (TsdA) that is widely distributed in bacteria. Mol Microbiol **88:**173-188.

62. **Chang DE, Smalley DJ, Tucker DL, Leatham MP, Norris WE, Stevenson SJ, Anderson AB, Grissom JE, Laux DC, Cohen PS, Conway T.** 2004. Carbon nutrition of Escherichia coli in the mouse intestine. Proc Natl Acad Sci U S A **101:**7427-7432.

63. **Clamp JR, Fraser G, Read AE.** 1981. Study of the carbohydrate content of mucus glycoproteins from normal and diseased colons. Clin Sci (Lond) **61:**229-234.

64. **Conway T, Krogfelt KA, Cohen PS.** 2004. The Life of Commensal Escherichia coli in the Mammalian Intestine. EcoSal Plus **1**.

65. **Corazziari ES.** 2009. Intestinal mucus barrier in normal and inflamed colon. J Pediatr Gastroenterol Nutr **48 Suppl 2:**S54-55.

66. **Fabich AJ, Jones SA, Chowdhury FZ, Cernosek A, Anderson A, Smalley D, McHargue JW, Hightower GA, Smith JT, Autieri SM, Leatham MP, Lins JJ, Allen RL, Laux DC, Cohen PS, Conway T.** 2008. Comparison of carbon nutrition for pathogenic and commensal Escherichia coli strains in the mouse intestine. Infect Immun **76:**1143-1152.

67. **Conway T, Cohen PS.** 2015. Commensal and Pathogenic Escherichia coli Metabolism in the Gut. Microbiol Spectr **3**.

68. **Maltby R, Leatham-Jensen MP, Gibson T, Cohen PS, Conway T.** 2013. Nutritional basis for colonization resistance by human commensal Escherichia coli strains HS and Nissle 1917 against E. coli O157:H7 in the mouse intestine. PLoS One **8:**e53957.

69. **Stecher B, Hardt WD.** 2011. Mechanisms controlling pathogen colonization of the gut. Curr Opin Microbiol **14:**82-91.

70. **Donaldson GP, Lee SM, Mazmanian SK.** 2015. Gut biogeography of the bacterial microbiota. Nat Rev Microbiol **14:**20-32.

71. **Schuster M, Lostroh CP, Ogi T, Greenberg EP.** 2003. Identification, timing, and signal specificity of Pseudomonas aeruginosa quorum-controlled genes: a transcriptome analysis. J Bacteriol **185:**2066-2079.

72. **Davenport PW, Griffin JL, Welch M.** 2015. Quorum Sensing Is Accompanied by Global Metabolic Changes in the Opportunistic Human Pathogen Pseudomonas aeruginosa. J Bacteriol **197:**2072-2082.

73. **Uzureau S, Lemaire J, Delaive E, Dieu M, Gaigneaux A, Raes M, De Bolle X, Letesson JJ.** 2010. Global analysis of quorum sensing targets in the intracellular pathogen Brucella melitensis 16 M. J Proteome Res **9:**3200-3217.

74. **Goo E, Majerczyk CD, An JH, Chandler JR, Seo YS, Ham H, Lim JY, Kim H, Lee B, Jang MS, Greenberg EP, Hwang I.** 2012. Bacterial quorum sensing, cooperativity, and anticipation of stationary-phase stress. Proc Natl Acad Sci U S A **109:**19775-19780.
75. **An JH, Goo E, Kim H, Seo YS, Hwang I.** 2014. Bacterial quorum sensing and metabolic slowing in a cooperative population. Proc Natl Acad Sci U S A **111:**14912-14917.
76. **Miyamoto CM, Meighen EA.** 2006. Involvement of LuxR, a quorum sensing regulator in *Vibrio harveyi*, in the promotion of metabolic genes: argA, purM, lysE and rluA. Biochim Biophys Acta **1759:**296-307.
77. **Studer SV, Mandel MJ, Ruby EG.** 2008. AinS quorum sensing regulates the Vibrio fischeri acetate switch. J Bacteriol **190:**5915-5923.
78. **Sun S, Tay QX, Kjelleberg S, Rice SA, McDougald D.** 2015. Quorum sensing-regulated chitin metabolism provides grazing resistance to *Vibrio cholerae* biofilms. ISME J **9:**1812-1820.
79. **Maddocks SE, Oyston PC.** 2008. Structure and function of the LysR-type transcriptional regulator (LTTR) family proteins. Microbiology **154:**3609-3623.
80. **Gallegos MT, Schleif R, Bairoch A, Hofmann K, Ramos JL.** 1997. Arac/XylS family of transcriptional regulators. Microbiol Mol Biol Rev **61:**393-410.
81. **Kelly A, Goldberg MD, Carroll RK, Danino V, Hinton JC, Dorman CJ.** 2004. A global role for Fis in the transcriptional control of metabolism and type III secretion in Salmonella enterica serovar Typhimurium. Microbiology **150:**2037-2053.
82. **Beisel CL, Storz G.** 2011. Discriminating tastes: physiological contributions of the Hfq-binding small RNA Spot 42 to catabolite repression. RNA Biol **8:**766-770.
83. **Beisel CL, Storz G.** 2012. The base-pairing RNA spot 42 participates in a multioutput feedforward loop to help enact catabolite repression in Escherichia coli. Mol Cell **41:**286-297.
84. **Hansen GA, Ahmad R, Hjerde E, Fenton CG, Willassen NP, Haugen P.** 2012. Expression profiling reveals Spot 42 small RNA as a key regulator in the central metabolism of Aliivibrio salmonicida. BMC Genomics **13:**37.
85. **Moller T, Franch T, Udesen C, Gerdes K, Valentin-Hansen P.** 2002. Spot 42 RNA mediates discoordinate expression of the E. coli galactose operon. Genes Dev **16:**1696-1706.
86. **Song T, Mika F, Lindmark B, Liu Z, Schild S, Bishop A, Zhu J, Camilli A, Johansson J, Vogel J, Wai SN.** 2008. A new *Vibrio cholerae* sRNA modulates colonization and affects release of outer membrane vesicles. Mol Microbiol **70:**100-111.
87. **Sabharwal D, Song T, Papenfort K, Wai SN.** 2015. The VrrA sRNA controls a stationary phase survival factor Vrp of *Vibrio cholerae*. RNA Biol **12:**186-196.
88. **Song T, Sabharwal D, Wai SN.** 2010. VrrA mediates Hfq-dependent regulation of OmpT synthesis in *Vibrio cholerae*. J Mol Biol **400:**682-688.

873 **Figure Legends**

874 **Fig. 1. Quorum sensing pathway in *V. parahaemolyticus*.** The sigma 54-dependent response
875 regulator LuxO activates the transcription of the quorum regulatory RNAs (*qrrs*) 1-5. These Qrrs
876 bind to the mRNA of the QS master regulators, blocking the translation of OpaR and promoting
877 the translation of AphA. OpaR and AphA repress the transcription of each other. In a *luxO*
878 mutant indicated by X, no *qrrs* are transcribed and this results in constitutive activation of OpaR
879 and repression of *aphA*. Dashed lines indicate no transcripts made and dashed arrows indicate no
880 regulation, solid lines indicate regulation, arrows indicate positive regulation and hammers
881 indicate negative regulation.

882 **Fig. 2**. ***In vivo* competition assays**. A 1:1 mixed culture of WBWlacZ and deletion mutants were
883 used to orogastrically infect streptomycin-pretreated adult mice. CFUs were calculated 24 h post
884 infection from the entire gastrointestinal tracts using a blue/white colony selection. Data are
885 pooled from two separate experiments and reported as competitive index (CI) for the *luxO* (n=8),
886 *aphA* (n=10), *opaR* (n=5), *luxO/opaR* (n=10), and *opaR/aphA* (n=7) mutants. The solid line
887 indicates the means. *P* values were calculated using a Welch's unpaired t-test with a 95%
888 confidence interval. Asterisks denote significant differences between the CI of the mutant strains
889 compared with the wild-type strain. *, $P < 0.05$; **, $P < 0.01$; ***, $P <= 0.001$ ****, $P < 0.0001$.

890 **Fig. 3. Expression analysis of quorum sensing master regulators and *qrrs***. RNA was
891 extracted from wild-type and mutant strains grown in M9 media supplemented with glucose
892 (M9G) to OD 1.0 and analyzed by qPCR in duplicate for each biological replicate. **A**. Bars
893 represent the expression of *opaR* normalized to 16S rRNA in the *luxO, rpoN* and *aphA* mutants
894 relative to wild-type cells. **B**. Bars represent the expression of the *aphA* normalized to 16S rRNA

895 in the *luxO, rpoN,* and *opaR* mutants relative to wild-type cells. **C.** Bars represent the expression
896 of *qrr 1, qrr2, qrr3* and *qrr5* normalized to 16S rRNA in Δ*luxO*. **D.** Bars represent the expression
897 of the *qrr 1, qrr2, qrr3* and *qrr5* normalized to 16S rRNA in Δ*rpoN*. *P* values were calculated
898 using an unpaired Student's t-test with a 95% confidence interval. Asterisks denote significant
899 differences in relative gene expression between mutant and wild-type. *, $P < 0.05$; **, $P < 0.01$.

900 **Fig. 4. QPCR validations of RNA Seq Expression in the *luxO* mutant relative to wild-type**.
901 Pre-ribozero treated RNA from the wild-type and the *luxO* mutant was used for cDNA synthesis
902 and expression analyzed by QPCR in duplicate for each biological replicate. **A**. Bars represent
903 the expression of the *opaR, aphA, qrr1, qrr2, qrr3 and qrr5* normalized to 16S rRNA in the *luxO*
904 mutant relative to wild-type cells. **B**. Bars represent the expression of four metabolism genes
905 normalized to 16S rRNA in the *luxO* mutant relative to wild-type. **C**. Bars represent relative
906 expression of T3SS and T6SS genes normalized to 16S rRNA in the *luxO* mutant relative to
907 wild-type cells. *P* values were calculated using an unpaired Student's t-test with a 95%
908 confidence interval. Asterisks denote significant differences in relative gene expression between
909 mutant and wild-type. *, $P < 0.05$; **, $P < 0.01$; ***, $P < 0.001$

910 **Fig. 5**. ***In vitro* competition assays of *V. parahaemolyticus* wild-type and the QS mutants**
911 ***luxO, opaR and aphA***. *In vitro* competition assays between the WBWlacZ strain and the mutant
912 strains in mucus and individual mucus sugars. *P* values were calculated using an unpaired
913 Student's t-test with a 95% confidence interval. Asterisks denote significant differences in CI
914 between the mutant strains and the wild-type. *, $P < 0.05$, **, $P < 0.01$, ***, $P < 0.001$

915 **Fig. 6. OpaR binding sites in regulatory regions of metabolism and transporter genes.**
916 Electrophoretic mobility shift assays (EMSAs) of the DNA fragments of promoter regions for

917 VP0008, VP1779, VPA1087, VPA0500, and VPA1424. Varying concentrations of OpaR (0 -3.7
918 μM) were incubated with DNA substrates corresponding to the promoter region of the following
919 genes starting upstream of the translational ATG start site; VP0008 (P*VP0008*: DNA probe 323-
920 bp), VP1779 (P*VP1779*: DNA probe 244-bp), VPA1087 (P*VPA1087*: DNA probe 333-bp),
921 VPA0500 (P*VPA0500)*: DNA probe 360-bp), and VPA1424 (P*VPA1424*: DNA probe 350-bp).
922 The DNA fragment from ORF VPA1667 (P*VPA1667*: DNA probe 308-bp) was used as a
923 negative control. Binding of OpaR was shown for all sites that were identified to contain putative
924 OpaR binding sites by bioinformatics. Ratios indicated above each gel image indicate ratio of
925 DNA: Protein concentrations used in each well. Grey arrows represent unbound DNA and black
926 arrows represent bound DNA. M=marker.

927

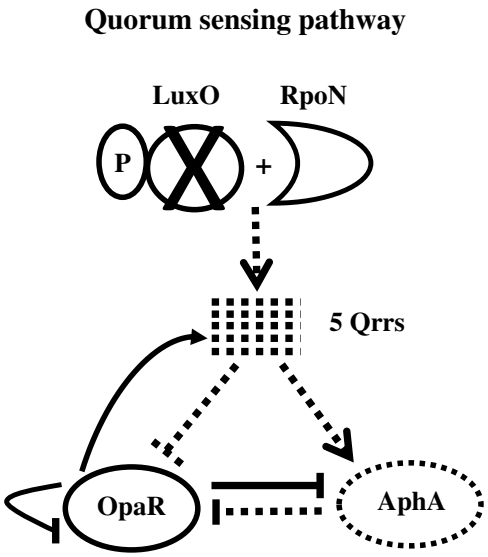

Fig. 1

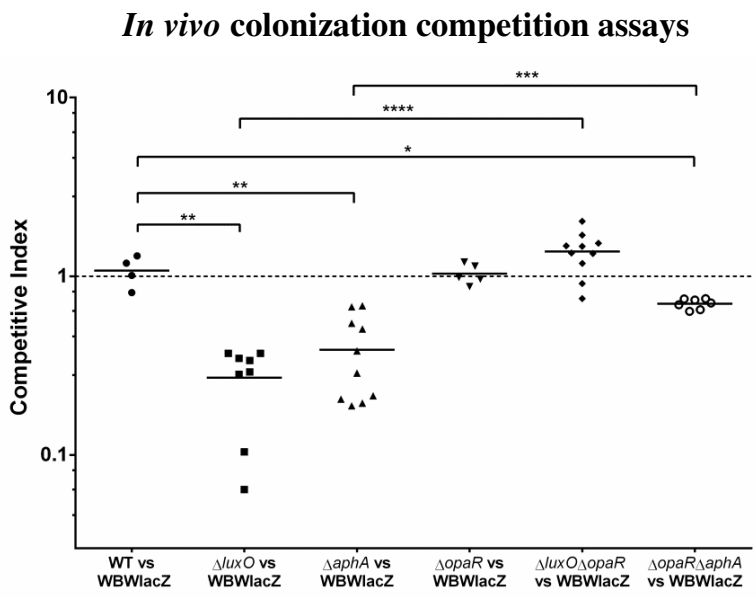

Fig. 2

A. Relative expression of *opaR*

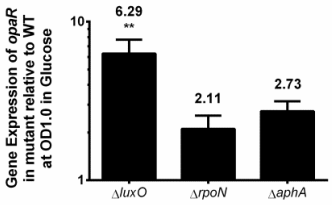

B. Relative expression of *aphA*

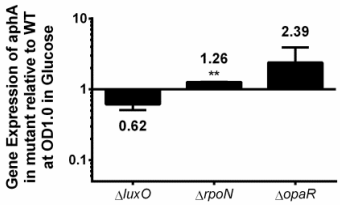

C. Relative expression of *qrrs* in Δ*luxO*

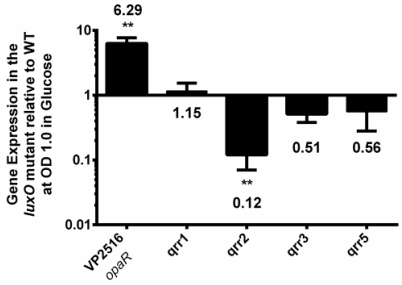

D. Relative expression of *qrrs* in Δ*rpoN*

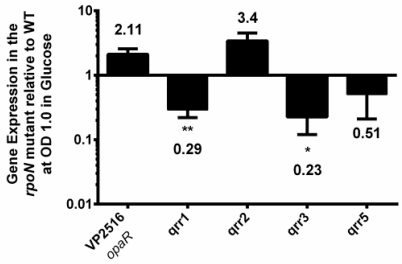

Fig. 3

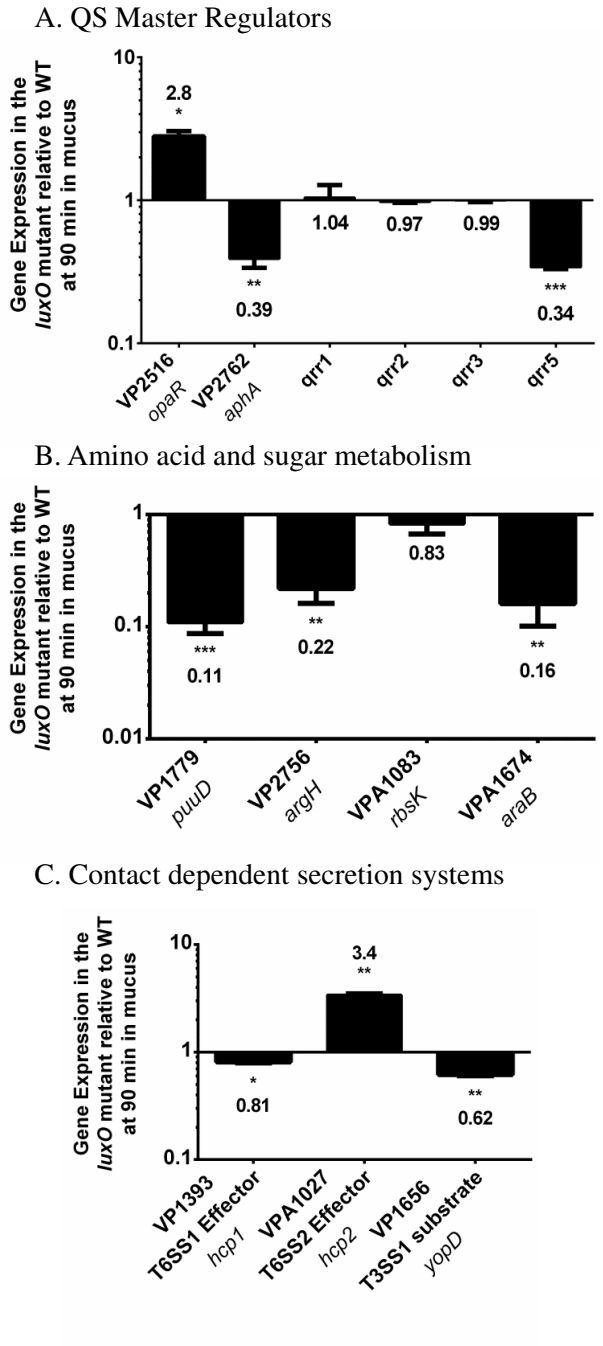

Fig. 4

In vitro competition assays

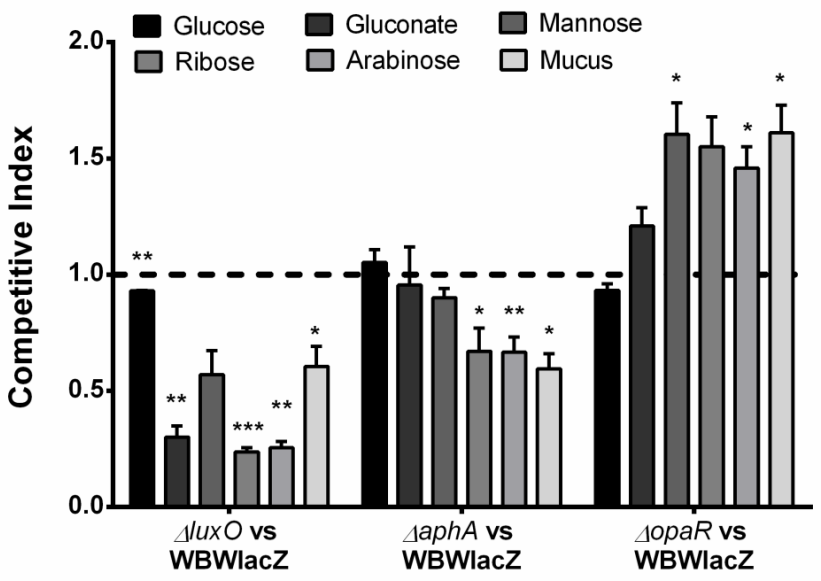

Fig. 5

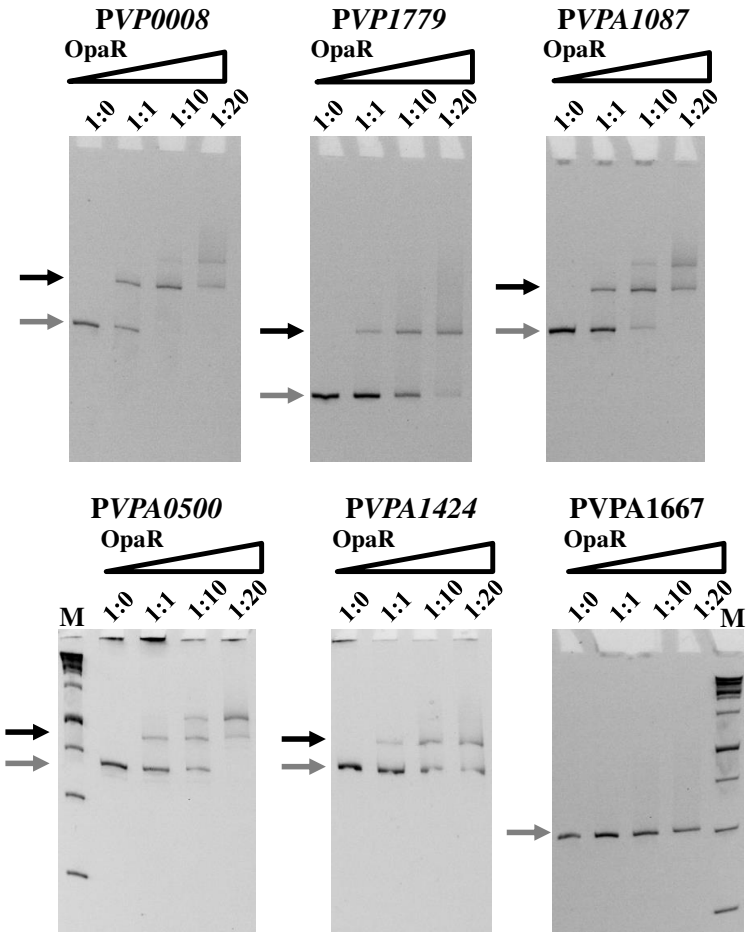

Fig. 6